

1 **Surface energy analysis (SEA) and rheology of powdered milk dairy products**

2
3 **Tubomir Lapčík**^{1,2*}, **Barbora Lapčíková**^{1,2}, **Eva Otyepková**¹, **Michal Otyepka**¹, **Jakub Vlček**¹,
4 **František Buňka**², **Richardos Nikolaos Salek**²

5
6 ¹ Department of Physical Chemistry, Regional Centre of Advanced Technologies and
7 Materials, Faculty of Science, Palacky University, 17. listopadu 12, 77146 Olomouc,
8 Czech Republic

9 ² **Tomas** Bata University in Zlin, Faculty of Technology, Institute of Foodstuff Technology,
10 nám. T.G. Masaryka 5555, 760 05 Zlín, Czech Republic

11
12 *Corresponding author.

13 E-mail address: lapcikl@seznam.cz, phone: +420732506770

14
15 **Key words:** skimmed milk powder, whey powder, demineralised whey powder, wetting,
16 surface energy distribution, surface energy analysis, inverse gas chromatography, thermal
17 analysis, scanning electron microscopy, powder rheology, flow index

18
19 **Abstract**

20 Results of inverse gas chromatography adsorption/desorption experiments **using** selected
21 probes on skimmed milk, whey and demineralised whey powder materials are presented. **The**
22 dispersive component of surface energy **was found to be dominant, indicating** low polarity
23 character. Surface energy profiles **of demineralised whey and skimmed milk showed a**
24 **characteristic** steep exponential decrease **from** approximately 170 mJ/m² to 60 mJ/m² **and**
25 **140 mJ/m² to 45 mJ/m², respectively, whereas whey powder exhibited a constant (non-**

26 **exponential) surface energy at** approximately 45 mJ/m²**. **The** dispersive surface energy of
27 **demineralised whey and skimmed milk powder showed a broad distribution** ranging
28 **from 40 mJ/m² to 120 mJ/m² and 175 mJ/m², respectively. In contrast, the dispersive**
29 surface energy distribution for whey **was very narrow, ranging** from **only** 42.8 mJ/m² to 45
30 mJ/m². **The determined** yield locus and Mohr's circles **indicated** that demineralised whey
31 **exhibited** free flowing powder characteristics, **whereas skimmed** milk and whey **exhibited**
32 **cohesive powder** flow behaviour.

33

34 **1. Introduction**

35

36 **Powdered** milk is a major precursor for many food products. Its value has been enhanced
37 **in recent years** by **the** relatively large amount of research **conducted to** support the
38 development and commercialisation of dairy-based products with an increasing variety of
39 **flavours, textures and shelf-lives** (Osorio, Monjes, Pinto, Ramirez, Simpson & Vega, 2014,
40 Saffari & Langrish, 2014, Crowley, Gazi, Kelly, Huppertz & O'Mahony, 2014, Bolenz,
41 Romisch & Wenker, 2014, Romeih, Abdel-Hamid & Awad, 2014, Martinez-Padilla, Garcia-
42 Mena, Casas-Alencaster & Sosa-Herrera, 2014, Zhou, Liu, Chen, Chen & Labuza, 2014,
43 Nilufer-Erdil, Serventi, Boyacioglu & Vodovotz, 2014). The colloidal nature of cow's milk is
44 a crucial structural feature that affects **its** final product quality as well as **processing**
45 behaviour (Fox & McSweeney, 1998, Gaucheron, Famelart, Mariette, Raulot, Michel &
46 Legraet, 1997). It can be divided into two compositional **domains: the** casein micelle and the
47 milk fat globule. These colloidal domains comprise nearly 80% of the approximate 12.7 g
48 total solids per 100 g⁻¹ in milk. **Therefore, investigation of** the structure and interactions of
49 these colloidal particles **continues** to be **an important area of** milk research. Dried milk
50 powders (e.g. whole, skimmed or retentate), dried buttermilk, and other dairy **powders (e.g.**

51 cheese whey powder (WP), whey protein concentrates (WPC), whey protein isolates (WPI),
52 caseinates and **lactose**) are products made from milk **or** whey where practically all the water
53 is removed, i.e. to $< 4 \text{ g per } 100 \text{ g}^{-1}$ of water (Tamime, Robinson & Michel, 2007). These
54 dried products have a very long shelf-life, they can be stored at ambient **temperature and** can
55 be **readily** exported to countries that have a shortfall in milk production. After rehydrating
56 milk powders, the reconstituted products may be similar to fresh milk (whole or **skimmed**),
57 **whereas the remaining** dairy powders have different applications in the dairy, food and
58 pharmaceutical industries.

59 In this **study, the** term skimmed milk powder defines a dairy product obtained by
60 removing the water from skimmed milk, with a maximum fat content of 11%, a maximum
61 moisture content of 5% and protein content not less than 31.4% of non-fatty dry extract.
62 Skimmed milk powder is by far the most important of **all milk powders** and the most widely
63 used form of milk protein in the food industry. Skimmed milk production firstly involves its
64 evaporation to a concentration of about 50% of total solids. Thereafter, the evaporated
65 skimmed milk can be dried in any of the various types of spray drier available. Two types of
66 powder **can** therefore **be distinguished: roller-dried powder** and spray-dried powder.
67 **Moreover, skimmed** milk powder **represents a** significant source of protein (35%) and
68 carbohydrate (lactose, 50%) and can be used as a food ingredient, for reconstitution and as an
69 animal feed. **As a food ingredient, it performs** three **main** functions: (i) contributes to a
70 desirable dairy flavour, (ii) affects food **texture, and** (iii) enhances the development of
71 desirable colour and flavour compounds (Tamime, Robinson & Michel, 2007, **Ranken, Kill**
72 **& Baker**, 1997).

73 Whey is a general term describing the translucent liquid part of milk that remains
74 following the process (isoelectric or rennet coagulation) of cheese manufacturing (Hoffman
75 & Falvo, 2004, Manso & Lopez-Fandino, 2004). Whey prepared by isoelectric precipitation

76 or rennet coagulation is called acid whey (dry whey with **0.35%** or higher titratable acidity on
77 a reconstituted basis) **or** sweet (rennet) whey (dry whey not over **0.16%** titratable acidity on a
78 reconstituted basis), respectively. Whey contains nearly 50% of the total solids found in
79 whole milk, including essentially **all the** lactose and whey proteins (Fundamentals of cheese,
80 15). The content of total essential amino acids and branched-chain amino acids is **high** in
81 whey protein than in most **other** dietary proteins (Helaine, Valdemiro, Dias, Borges, &
82 Tanikawa, 2001). Whey and whey products are commonly used in animal feed, dietetic foods
83 (infant food), bread, confectionery, candies and beverages. The composition of whey products
84 varies depending on several factors, including the source of the milk, production method, type
85 of cheese **and** manufacturer's specifications. Whey and whey components contain a number
86 of valuable minerals **such as calcium, magnesium, manganese, phosphorus, copper, iron,**
87 **zinc, sodium and potassium.**

88 The main component of whey is lactose (**70-75%**), **while** the major component of
89 whey solids **are** whey proteins (**10-13%**), **mainly** lactalbumin and globulins. Practically all
90 the mineral elements found in whey are essential for nutrition. Condensed whey, dried whey,
91 dried modified whey, whey protein concentrate and isolates, as well as lactose (**crystallised**
92 and dried) are the **most** often **reported** whey products. Whey can also be processed into a
93 number of valuable **products**, as well as some that are considered waste products. **Examples**
94 **of** whey types include reduced lactose whey, demineralised whey, acid **whey**, **sweet** whey and
95 whey protein concentrate. Whey protein is a complete, high quality protein with a rich amino
96 acid profile. Whey proteins refer to a group of individual proteins or fractions that separate
97 out **from casein** during cheese-making. These fractions are **usually** purified to different
98 **concentrations depending** on the end composition desired **and vary** in their content of
99 protein, lactose, carbohydrates, **immunoglobulins**, minerals and fat (Tamime et al., 2007).

100 Demineralised whey powder is produced from whey by selective removal of most of the
101 minerals.

102 The properties of surfaces and interfaces **characterised** by surface or interfacial
103 tension and surface energy **have attracted increasing attention** in recent years. **Such**
104 properties **affect** many phenomena **associated with** adhesion, wetting, spreading and
105 **wicking, which play an important role in everyday** life, natural processes **and numerous**
106 industrial applications. These processes **are important in** various **materials, for** instance
107 biopolymers (Lapčik, Lapčik, De Smedt, Demeester & Chabreček, 1998, Collins, 2014),
108 synthetic polymers, wood (Lapčik, Lapčik, Kubiček, Lapčíková, Zbotil & Nevečná, 2014),
109 paper, stone, soils (Lapčik, Lapčíková, Krásný, Kupská, Greenwood & Waters, 2012),
110 cereals and **textiles, encompassing** all possible types of surface **from polar to non-polar**
111 **(Gamble et al., 2012). However, the surfaces of such materials are usually rough rather**
112 **than smooth and may even be porous, making their surface characterisation challenging.**
113 Despite the **difficulties, several methods are applicable for characterising** powder and
114 fibrous materials (Gajdošíková, Lapčíková & Lapčik, 2011), such as **the** capillary rise
115 method, thin-layer wicking **and Wilhelmy** plate method. **In particular, a surface energy**
116 analysis technique based on inverse gas chromatography has been found to be very effective
117 **for characterising** wetting phenomena on powders and fibres (Mohammadi-Jam & Waters,
118 2014, Lapčik, Otyepková, Lapčíková & Otyepka, 2013, Lazar, P. et al., 2014)

119

120

121 **2. Methods**

122 ***2.1.Theoretical background***

123 **The surface** free energy of a solid can be described **by** the sum **of dispersive** and
124 specific contributions. Dispersive (apolar) interactions, also known as Lifshitz-van der Waals

125 interactions, consist of London **interactions originating** from electron density changes but
 126 may **also** include both Keesom and Debye interactions (Gajdošíková et al, 2011). Other forces
 127 influencing the magnitude of surface energy are Lewis acid-base **interactions, which** are
 128 generated between **an** electron acceptor (acid) and electron donor (base). They **occur in**
 129 **compounds** containing hydrogen bonds - strong secondary bonds between atoms of hydrogen
 130 and a highly electronegative element such as F, O, N and Cl or other compounds **that can**
 131 **interact with** Lewis acids and bases. Details of the **most** widely accepted theoretical
 132 treatment **for estimation** of solid surface free **energies from** selective wetting measurements
 133 are **given** in our **recent** review article (Gajdošíková et al., 2011).

134 The dispersive component of the surface energy γ_S^D can be calculated from the
 135 retention **times** obtained from inverse gas chromatography measurements of a series of n-
 136 alkane probes injected at infinite dilution (concentration within the **Henry region** of the
 137 adsorption **isotherm**) (Belgacem, Gandini & Pefferkorn, 1999). For evaluation of these
 138 **dependencies, two approaches have been used, as described by Equations (1)** (Schultz,
 139 Lavielle & Martin, 1987) **and (2) (Dorris & Gray, 1980):**

140

$$141 \quad RT \ln V_N = a (\gamma_L^D)^{1/2} 2N_A (\gamma_S^D)^{1/2} + C \quad (1)$$

142

143 where R is the universal gas constant, N_A is Avogadro's number, γ_L^D is the dispersive
 144 component of surface free energy of the liquid probe, γ_S^D is the dispersive component of the
 145 surface free energy of the solid, V_N is the retention volume and C is a constant, and

146

$$147 \quad \gamma_S^D = \frac{RT \ln \left(\frac{V_{N^{C_nH_{2n+4}}}}{V_{N^{C_nH_{2n+2}}} \right)}{4 N_A^2 a_{CH_2}^2 \gamma_{CH_2}} \quad (2)$$

148

149 where a_{CH_2} is the surface area of a CH_2 unit ($\sim 0.6 \text{ nm}^2$) and γ'_{CH_2} is its free energy
150 (approximately **35.6 mJ/m²**).

151

152 ***2.2.Experimental***

153

154 Inverse gas chromatography was conducted using a **surface energy analyser** (SEA) (Surface
155 Measurement Systems, UK). Samples were placed in 4 mm (internal diameter) **columns to**
156 give a total surface area of approximately 0.5 m^2 . The following eluent vapours were passed
157 through the column: **nonane, octane, hexane and heptane**. All reagents were obtained from
158 Sigma Aldrich (**USA**) and were of analytical grade. The injection of vapours was controlled
159 **in order** to pass a set volume of eluent through the column to give pre-determined fractional
160 coverage of the sample in the column. **Using this method, the** retention time of the vapours
161 **through** the particles gives an indication of the surface properties of the material, including
162 the surface energy. By gradually increasing the amount of vapour injected, it is possible to
163 build up a surface heterogeneity plot.

164 Specific surface area measurements were made using a Micromeritics TriStar 3000
165 surface area and porosity analyser (USA) **combined with** the nitrogen BET technique.

166 Thermogravimetry (TG) and differential thermal analysis (DTA) experiments were
167 performed on a Netzsch STA 449 C Jupiter **simultaneous thermal analyser** (Netzsch,
168 Germany). **Samples were weighted to aluminium pans and measured. Each measurement**
169 **was repeated 3 ×. Conditions of measurement: Heat flow 10 °C/min and dynamic**
170 **atmosphere of nitrogen (N₂ 50 ml/min), range of temperature measurement was from**
171 **35 °C to 300 °C**. Throughout the experiment, the sample temperature and weight-heat flow
172 changes were continuously monitored.

173 Scanning electron microscopy (SEM) images were captured on a Hitachi 6600 FEG
174 microscope (Japan) operating in the secondary electron mode and using an accelerating
175 voltage of 1 kV.

176 Powder rheology measurements were **acquired** on a FT4 Powder rheometer (Freeman
177 Technology, UK). All experiments were performed **under the** laboratory ambient
178 temperature of **23 °C** and air relative humidity of **43%**.

179 **The moisture content of the powdered samples was as follows:** skimmed **milk 3.7**
180 **wt.%, whey 2.0 wt.% and demineralised whey 2.4 wt.%** (Moravia Lacto, Czech
181 Republic). **The powdered** milk samples were **stored under** dry conditions in desiccators (at
182 **an ambient temperature of 23 °C**) for 2 weeks prior to **the** experiments.

183

184 **3. Results and discussion**

185

186 A typical SEM **image for the powdered** milk materials under study **is presented** in
187 Figure 1, **showing that the particles had a spherical shape. The** individual **particle**
188 diameter of **the powdered** skimmed milk **sample** was found to be 15.1 μm , **compared to**
189 80.0 μm and **88.0 μm** for **the powdered whey and** demineralised whey **samples,**
190 **respectively.** All samples were characterised by thermogravimetric and DSC measurements
191 **over a** temperature range of +35 to +300 °C to evaluate moisture content and thermal
192 stability. **The observed** TG and DSC temperature dependencies are shown in Figures 2 and 3.
193 **It can be seen from these scans (Figure 2) that the powdered** skimmed milk **and whey**
194 samples **exhibited** three step weight loss patterns. **The first** TG weight loss step **occurred**
195 **from 35 to 150 °C and corresponded to a** weight loss of 4.6 **wt.%** for **the** skimmed milk
196 **and 3.1 wt.%** for **the whey sample, representing** moisture release of physically retained
197 water molecules by casein or whey proteins. **As** all samples were conditioned **at the same**

198 **humidity** prior to the experiments, **the** linear zero moisture behaviour in the case of
199 demineralised whey **is likely due** to its low **mineral** content in comparison to the other two
200 materials (**skimmed** milk and whey). **The second** TG degradation step **occurring over the**
201 **temperature range 150 to 248 °C** was **attributed** to the thermo-destruction of casein and
202 whey **proteins** (Mocanu, Moldoveanu, Odochian, Paius, Apostolescu & Neculau, 2012). The
203 thermal stability of **the** studied milk dairy products **can be described** by the initial
204 temperature of thermal degradation (**2. region**), **which was** 150 °C. **At this temperature, the**
205 weight loss for all samples was approximately 25 to 32 **wt.%**. The third degradation step was
206 initiated at 248 °C for **skimmed** milk and whey and at 236 °C for demineralised whey. **The**
207 residual masses were 62.9 **wt.%** for **powdered** skimmed milk, 56.9 **wt.%** for **powdered**
208 whey and 60.9 **wt.%** for demineralised **powdered** whey. As evident from Figure 2, the
209 weight lost **pattern** of skimmed milk **during the third degradation step** was inverted
210 (**became** the lowest) in comparison to the first and second degradation regions. We ascribed
211 this behaviour to the higher residual mass of lactose in comparison to the milk fats. **The**
212 **thermal** characteristics of milk powder are significantly affected by fat and lactose content
213 (**Rahman, Al-Hakmani, Al-Alawi & Al-Marhubi**, 2012). However, the tangent of the
214 sample weight at 200 °C **was** higher for the whey products in comparison to the skimmed
215 milk, **indicating that milk fats have a** lower degradation **resistivity in** comparison **to lactose**
216 **in** skimmed milk. **As milk** is a multi-component **mixture, it** would be difficult to **attribute**
217 its thermal **behaviour to particular** components **as** complex individual as well as synergistic
218 effects **need to be taken into account**.

219 Based on **the** DSC data (Figure **3**), **the** first exothermic peak at approximately 170 °C can
220 be **assigned to lactose crystallisation** and **the** second **huge peak** to the non-enzymatic
221 browning advanced Maillard reaction between proteins and **lactose, which is** initiated at a
222 temperature of 220 °C (Vuataz, Meunier & Andrieux, 2010, **Rahman et al.**, 2012)). The last

223 third degradation region **is likely to correspond to oxidation** of milk fats **and lactose**
224 degradation (Raemy, Hurrell & Löliger, 1983).

225 **The specific** surface areas of the studied samples were identical for all materials under
226 **study. Although the** obtained value of $0.6 \text{ m}^2/\text{g}$ was relatively low, **it was** in excellent
227 agreement **with data** available in **previous** literature (Berlin, Howard & Pallansch, 1964).

228 Surface energy profiles and their components of **the** studied milk products powders based
229 on **the** inverse gas chromatography **measurements are** shown in Figure 4. **The** surface
230 energy profiles of **skimmed** milk and demineralised whey **clearly differed from that of**
231 **whey. The** first two materials (**skimmed** milk and demineralised whey) **showed a**
232 **characteristic steep** exponential decrease in surface energy **from approximately 170 mJ/m^2**
233 **to 60 mJ/m^2 and 140 mJ/m^2 to 45 mJ/m^2 , respectively, between a coverage of 0% to**
234 **approximately 2% (skimmed milk) and 5% (demineralised whey), reflecting the**
235 relatively **low** number of high energy sites **on** the surface of **these** materials. **In contrast, for**
236 **a surface coverage of 5% up to 20%, the** surface energy **profiles plateaued** at 45 mJ/m^2
237 (**skimmed milk**) and 60 mJ/m^2 (**demineralised whey**). As clearly visible from Figure 4, **the**
238 dispersive component **dominated the** surface **energy, thus** reflecting **the** non-polar nature of
239 the surface active sites in **both skimmed** milk and demineralised **whey powders**. The same
240 hydrophobic character was **also found for** the third material under **study, i.e.** whey. However,
241 in contrary to the above mentioned skim milk and demineralised whey materials, a surface
242 energy coverage dependence exhibited stable non-exponential (linear) pattern with the
243 magnitude of the observed surface energy approximately 45 mJ/m^2 , thus reflecting high
244 homogeneity of acting energetic surface sites**. For all three tested materials, **the** polar
245 component of the surface energy was negligible in comparison to the dispersive component.
246 **For both the whey and demineralised whey powders, its value** was **independent of**
247 **coverage at approximately 5 mJ/m^2 , thus suggesting a** high uniformity of surface structural

248 components responsible for this kind of behaviour. **However, the polar component of**
249 **skimmed milk showed an exponential decay, ranging from 30 mJ/m² for a coverage of**
250 **0% coverage up to 5 mJ/m² for coverages of 3% up to 20%, which indicates a** broader
251 distribution **of energetic** sites responsible for such behaviour due to the **increased** complexity
252 of the main **milk constituents. It was also evident that** the polar surface active sites **were** of
253 relatively low energy in all **the** studied powders, **providing further evidence of** their low
254 polarity character. Such behaviour can be attributed to the presence **of milk** fat components at
255 the surface interface (Jensen, Ferris & Lammi-Keefe, 1991).

256 **The measured** dispersive surface energy (Figure 5), **showed a characteristically** broad
257 **distribution for both skimmed milk (40 mJ/m² to 175 mJ/m²) and demineralised whey (40**
258 **mJ/m² to 120 mJ/m²), thus reflecting the large** number of structural elements responsible for
259 this behaviour. **However,** the dispersive surface energy distribution **of** whey **was** very
260 **narrow (see Figure 5 - inset), ranging from only 42.8 mJ/m² to 45 mJ/m², with** relatively
261 the same area increment occupancy of 2% as for demineralised whey. **In contrast, the area**
262 increment occupancy for **skimmed** milk was 3 times **higher, reaching 6%. This SEA pattern**
263 behaviour **may be due to** the **greater concentration** of inorganic salts in whey in comparison
264 **to milk** and demineralised whey, which might successfully screen the most energetic **surface**
265 **sites** (at the lowest surface coverage) by binding surrounding water molecules remaining as
266 residual moisture content.

267 **The** macroscopic powder flow behaviour **was also investigated by determining the**
268 yield locus and flow function dependencies at different stress levels for **the** studied **samples.**
269 Results of the powder rheological measurements are shown in Figure 6, **which presents the**
270 yield locus and Mohr's circles of **the** tested powder milk dairy products. **The results show**
271 that demineralised whey exhibited free flowing powder **characteristics, as indicated by the**
272 observed friction coefficient **of 11.7. In contrast, the friction** coefficients of **the skimmed**

273 milk and whey powders **ranged from 3.3** to 4.5, **which are** values characteristic for cohesive
274 powders behaviour. **The** unconfined yield strengths **ranged** from 1.37 kPa (demineralised
275 whey) to 4.48 kPa (**skimmed** milk) and 4.69 kPa (whey). The unconfined yield **strength**, σ_c ,
276 **can be obtained** from the stress circle tangential to the yield locus **and passing** through the
277 origin (minor principal stress $\sigma_2 = 0$). Because the largest Mohr stress circle **indicated** a state
278 of steady-state flow, the internal friction angle can be regarded as a measure of the internal
279 friction at steady-state flow (**Lapčík et al.**, 2012). For **the** studied **samples**, **the** angle of
280 internal friction **ranged** from **26.5°** for whey up to 36.4 and **40.4°** for demineralised whey and
281 **skimmed milk, respectively**. **The** **relatively** low value of the angle of internal friction
282 observed for whey **is consistent with** the observed friction factor of 3.3 characteristic for
283 cohesive powders. The relevant consolidation **stress**, σ_1 , **can be obtained from** the major
284 principal stress of the Mohr stress **circle tangential** to the yield locus and **intersecting** the
285 point of steady flow. **The major principle** stress for all **the** tested powders was about 16 to
286 18 kPa. The latter stress circle represents the stresses in the sample at the end of the
287 consolidation procedure (stress at steady state flow). It corresponds to the stress circle at the
288 end of consolidation **in** the uniaxial compression test.

289 In addition to the above shear **testing, powder** aeration tests were performed, allowing
290 consideration of the fluidisation capability of the studied powders. **The** aeration ratio **was**
291 **found to range** from 32.4 for whey to 12.7 (demineralised whey) and 8.98 for **skimmed**
292 **milk, whereas the** aerated **energy varied** from 4.8 mJ (whey) to 10.1 mJ (demineralised
293 whey) and 14.4 mJ (**skimmed** milk). **The** aeration data **indicated** that **whey showed the**
294 **lowest cohesion of all the samples tested, i.e.** highest aeration **ratio** in combination with the
295 lowest aerated energy. All **the** tested powders **exhibited** complete fluidisation **at 4** mm/s air
296 **velocity, with** basic flowability energy ranging from 127 mJ (**skimmed** milk and
297 demineralised whey) to 157 mJ for whey.

298

299 **Conclusions**

300

301 **The results showed that the surface energy of the studied milk product powders was**
302 **dominated by the dispersive component, indicating their low polarity character.** Surface
303 energy profiles of **skimmed** milk and demineralised whey **showed a characteristic steep**
304 exponential decrease of the surface energy from approximately 170 mJ/m² to 60 mJ/m²
305 (demineralised whey) and of 140 mJ/m² to 45 mJ/m² (**skimmed milk**), **reflecting the**
306 relatively **small** number of high energy sites located at the surface of the studied materials.
307 **From 5% up to 20% surface coverage, the surface energy profiles reached a plateau** at 45
308 mJ/m² for **skimmed** milk and 60 mJ/m² for demineralised **whey**. **Whey** powder surface
309 energy coverage dependence exhibited stable non-exponential (linear) pattern with the
310 magnitude of the observed surface energy approximately 45 mJ/m², thus reflecting high
311 homogeneity of acting energetic surface sites. For all three tested materials, **the polar**
312 component of the surface energy was negligible in comparison to the dispersive component. It
313 was **found that** the polar surface active sites **were** of relatively low energy in all **the** studied
314 powders, **confirming** their low polarity character. **The observed** dispersive surface energy
315 **showed characteristically broad** distributions for **skimmed** milk and demineralised whey
316 ranging from 40 mJ/m² to **175** mJ/m² and **120** mJ/m², **respectively**, thus reflecting **the large**
317 number of structural elements responsible for this behaviour. **In contrast, the dispersive**
318 surface energy distribution **of whey was very narrow, ranging from only** 42.8 mJ/m² to 45
319 mJ/m². **The macroscopic** powder flow behaviour of **the** studied materials **was analysed by**
320 **examining the** yield locus and flow function dependencies at different stress levels. **The**
321 **determined** yield locus and Mohr's circles **indicated** that demineralised whey exhibited free
322 flowing powder characteristics (observed friction coefficient 11.7). However, **the friction**

323 coefficients of **the skimmed** milk and whey powders were in the **range 3.3** to 4.5, **which are**
324 values characteristic for cohesive **powders**. All tested powders **allowed** complete fluidisation
325 **at 4 mm/s** air **velocity**, **with** basic flowability **energies** ranging from 127 mJ (**skimmed** milk
326 and demineralised whey) to 157 mJ for whey.

327

328 **Acknowledgements**

329 Financial support from the Operational Program Research and Development for Innovations –
330 European Regional Development Fund (grants CZ.1.05/3.1.00/14.0302 and
331 CZ.1.05/2.1.00/03.0058) and **the** Tomas Bata University in Zlin and Palacky University in
332 Olomouc Internal Grant Agencies (projects IGA/FT/2014/001 and PrF_2014_032) is
333 gratefully acknowledged. Special thanks to Mgr. K. Šafářová, Ph.D. for **performing the SEM**
334 measurements.

335

336 **References**

337 Belgacem, M.N., Gandini, **A.**, & Pefferkorn, M.N. (1999). Interfacial phenomena in chro-
338 matography. New York: Marcel Dekker.

339 Berlin, E., Howard, **N.M.**, & Pallansch, M.J. (1964). Specific surface area of milk powders
340 produced by different drying methods. *Journal of Dairy Science*, **47**, **132–138**.

341 Bolenz, S., Romisch, **J.**, & Wenker, T. (2014). Impact of amorphous and crystalline lactose
342 on milk chocolate properties. *International Journal of Food Science and Technology*, **49**,
343 **1644–1653**.

344 Collins, M.N. (2014). Hyaluronic acid biomedical and pharmaceutical applications.
345 Shawbury: Smithers Rapra.

346 Crowley, S.V., Gazi, I., Kelly, A.L., Huppertz, T., & O'Mahony, J.A. (2014). Influence of
347 protein concentration on the physical characteristics and flow properties of milk protein
348 concentrate powders. *Journal of Food Engineering*, **135**, 31–38.

349 Dorris, G.M., & Gray, D.G. (1980). Adsorption of normal-alkanes at zero surface coverage
350 on cellulose paper and wood fibers. *Journal of Colloid and Interface Science*, **77**, 353–362.

351 Fox, P.F., & McSweeney, P.L.H. (1998). Dairy chemistry and biochemistry. New York:
352 Kluwer Academic/Plenum Publishers.

353 Gajdošíková, R., Lapčíková, B., & Lapčík, L. (2011). Surface phenomena and wetting of
354 porous solids. *Physical Chemistry: An Indian Journal*, **6**, 146–162.

355 Gamble, J.F., Leane, M., Olusanmi, D., Tobyn, M., Supuk, E., Khoo, J., & Naderi, M.
356 (2012). Surface energy analysis as a tool to probe the surface energy characteristics of
357 micronized materials – a comparison with inverse gas chromatography. *International Journal
358 of Pharmaceutics*, **422**, 238–244.

359 Gauchon, F., Famelart, M.H., Mariette, F., Raulot, K., Michel, F., & LeGraet, Y. (1997).
360 Combined effects of temperature and high-pressure treatments on physicochemical
361 characteristics of skim milk. *Food Chemistry*, **59**, 439–447.

362 Helaine, B.J., Valdemiro, C.S., Dias, N.F.G.P., Borges, P., & Tanikawa, C. (2001). Impact of
363 different dietary protein on rat growth, blood serum lipids and protein and liver cholesterol.
364 *Nutrition Research*, **21**, 905–915.

365 Hoffman, **J.R.**, & Falvo, M.J. (2004). Protein – Which is best? *Journal of Sports Science and*
366 *Medicine*, **3**, **118 130**.

367 Jensen, R.G., Ferris, **A.M.**, & Lammi-Keefe, C.J. (1991). The composition of milk fat.
368 *Journal of Dairy Science*, **74**, **3228 3243**.

369 Lapčík, L., Lapčík, L., De Smedt, S., Demeester, **J.**, & Chabreček, P. (1998). Hyaluronan.
370 preparation, structure, properties and applications. *Chemical Reviews*, **98**, **2663 2684**.

371 Lapčík, L., Lapčík, L., Kubiček, P., Lapčíková, B., Zbořil, **R.**, & Nevěčná, T. (2014) Study
372 of penetration kinetics of sodium hydroxide aqueous solution into wood samples.
373 *BioResources*, **9**, **881 893**.

374 Lapčík, L., Lapčíková, B., Krásný, I., Kupská, I., Greenwood, **R.W.**, & Waters, K.E. (2012).
375 Effect of low temperature air plasma treatment on **wetting** and flow properties of kaolinite
376 powders. *Plasma Chemistry and Plasma Processing*, **32**, **845 858**.

377 Lapčík, L., Otyepková, E., Lapčíková, **B.**, & Otyepka, M. (2013). Surface energy analysis
378 (SEA) study of hyaluronan powders. *Colloids and Surfaces A: Physicochemical and*
379 *Engineering Aspects*, **436**, **1170 1174**.

380 Lazar, P., Otyepková, E., Banaš, P., Fargašová, A., Šafářová, K., Lapčík, L., Pechoušek,
381 Zbořil, **R.**, & Otyepka, M. (2014). The nature of high surface energy sites in graphene and
382 graphite. *Carbon*, **73**, **448 453**.

383 Manso, **M.A.**, & Lopez-Fadino, R. (2004). j-Casein macropeptides from cheese whey:
384 Physicochemical, biological, nutritional, and technological features for possible uses. *Food*
385 *Reviews International*, **20**, **329 355**.

386 Martinez-Padilla, L.P., Garcia-Mena, V., Casas-Alencaster, **N.B.**, & Sosa-Herrera, M.G.
387 (2014). Foaming properties of skim milk powder fortified with milk proteins. *International*
388 *Dairy Journal*, **36**, **21** **28**.

389 Mocanu, A.M., Moldoveanu, C., Odochian, L., Paius, C.M., Apostolescu, **N.**, & Neculau, R.
390 (2012). Study on the thermal behaviour of casein under nitrogen and air atmosphere by means
391 of the TG-FTIR technique. *Thermochimica Acta*, **546**, **120** **126**.

392 Mohammadi-Jam, **S.**, & Waters, K.E. (2014). Inverse chromatography applications: A
393 review. *Advances in Colloid and Interface Science*,
394 <http://dx.doi.org/10.1016/j.cis.2014.07.002>.

395 Nilufer-Erdil, D., Serventi, L., Boyacioglu, **D.**, & Vodovotz, Y. (2012). Effect of soy milk
396 powder addition on staling of soy bread. *Food Chemistry*, **131**, **1132** **1139**.

397 Osorio, J., Monjes, J., Pinto, M., Ramirez, **C.**, **Simpson, R.**, & Vega, O. (2014). Effects of
398 spray drying conditions and the addition of surfactants on the foaming properties of a whey
399 protein concentrate. *LWT-Food Science and Technology*, **58**, **109** **115**.

400 Raemy, A., Hurrell, **R.F.**, & Löliger, J. (1983). Thermal behavior of milk powders studied by
401 differential thermal analysis and heat flow calorimetry. *Thermochimica Acta*, **65**, **81** **92**.

402 Rahman M.S., Al-Hakmani, H., Al-Alawi, **A.**, & Al-Marhubi, I. (2012). *Thermochimica Acta*,
403 **549**, **116** **123**.

404 Ranken, M.D., Kill, **K.C.**, & Baker, C. (1997). **Food industrial manual**. London: Blackie
405 Academic & Professional.

406 Romeih, E.A., Abdel-Hamid, **M.**, & Awad, A.A. (2014). The addition of buttermilk powder
407 and transglutaminase improves textural and organoleptic properties of fat-free buffalo yogurt.
408 *Dairy Science & Technology*, **94**, 297 309.

409 Saffari, **M.**, & Langrish, T. (2014). Effect of lactic acid in-process crystallization of
410 lactose/protein powders during spray drying. *Journal of Food Engineering*, **137**, 88 94.

411 Schultz, L., Lavielle, **C.**, & Martin, J. (1987). The role of **the** interface in carbon fibre-epoxy
412 composites. *Journal of Adhesion*, **23**, 45 60.

413 Tamime, A.Y., Robinson, **R.K.**, & Michel, M. (2007). Microstructure of concentrated and
414 dried milk products. In A.Y. Tamime (Ed.), *Structure of dairy products* (pp. 104 133).
415 Oxford: Blackwell Publishing Ltd.

416 Vuataz, G., Meunier, **V.**, & Andrieux, J.C. (2010). Tg-DTA approach for designing reference
417 methods for moisture content determined in food powders. *Food Chemistry*, **122**, 436 442.

418 Zhou, P., Liu, D.S., Chen, X.X., Chen, **Y.J.**, & Labuza, T.P. (2014). Stability of whey protein
419 hydrolysate powders: Effects of relative humidity and temperature. *Food Chemistry*, **150**,
420 457 462.

421

422 **Figures captions**

423

424 Figure 1. SEM images of studied powders: A) skimmed milk, B) **whey**, and C) demineralised
425 whey.

426 Figure 2. Thermogravimetric **analysis of** studied powder milk products: full line – **powdered**
427 skimmed milk, **dotted** line **powdered** whey, short dashed line – demineralised **powdered**
428 whey.

429 Figure 3. DSC pattern of studied powder milk products: full line – **powdered** skimmed milk,
430 dot line – **powdered** whey, short dashed line – demineralised **powdered** whey.

431 Figure 4. Surface energy and its **component** profiles **of powdered** milk products: circle –
432 **powdered** whey, **triangle** – demineralised **powdered** whey, diamond – **powdered skimmed**
433 **milk**, **black**– dispersive component of the surface energy (SFE), **red** polar component of
434 **SFE**, **green** colour – total SFE.

435 Figure 5. Dispersive surface energy distribution **of** demineralised **powdered** whey (circle),
436 **powdered skimmed** milk (triangle down) and **powdered** whey (triangle up). **Inset:**
437 **expanded** dispersive surface energy distribution **of** whey sample.

438 Figure 6. Yield locus and Mohr's circles of studied **powdered** milk products: full square –
439 **skimmed** milk, full triangle up whey, empty circle demineralised whey (measured at 24
440 °C).

441

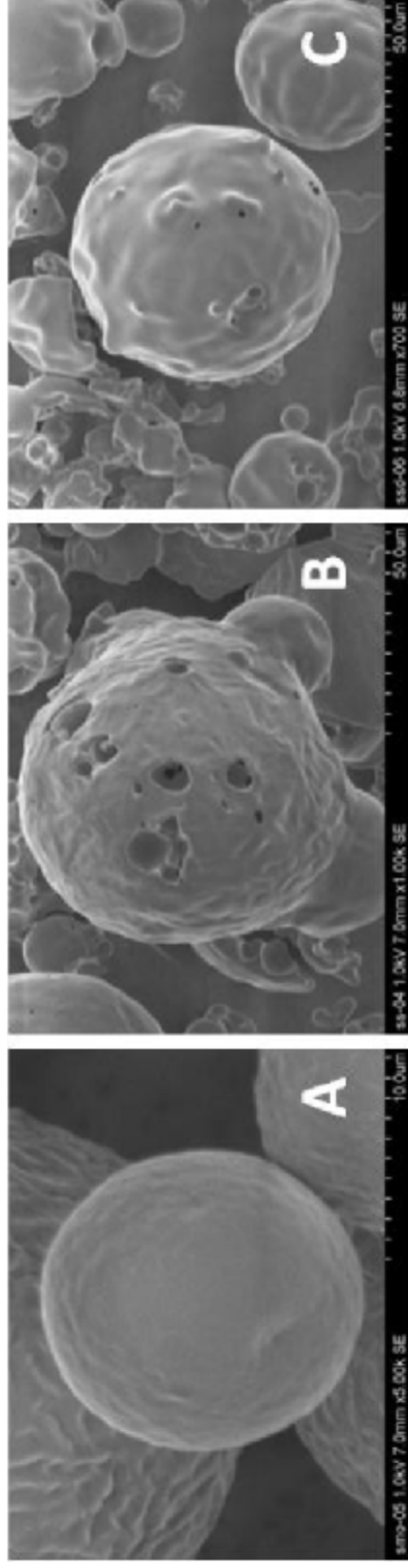


Figure 1. SEM images of studied powders: A) skimmed milk, B) whey, and C) demineralised whey.

Figure(s)

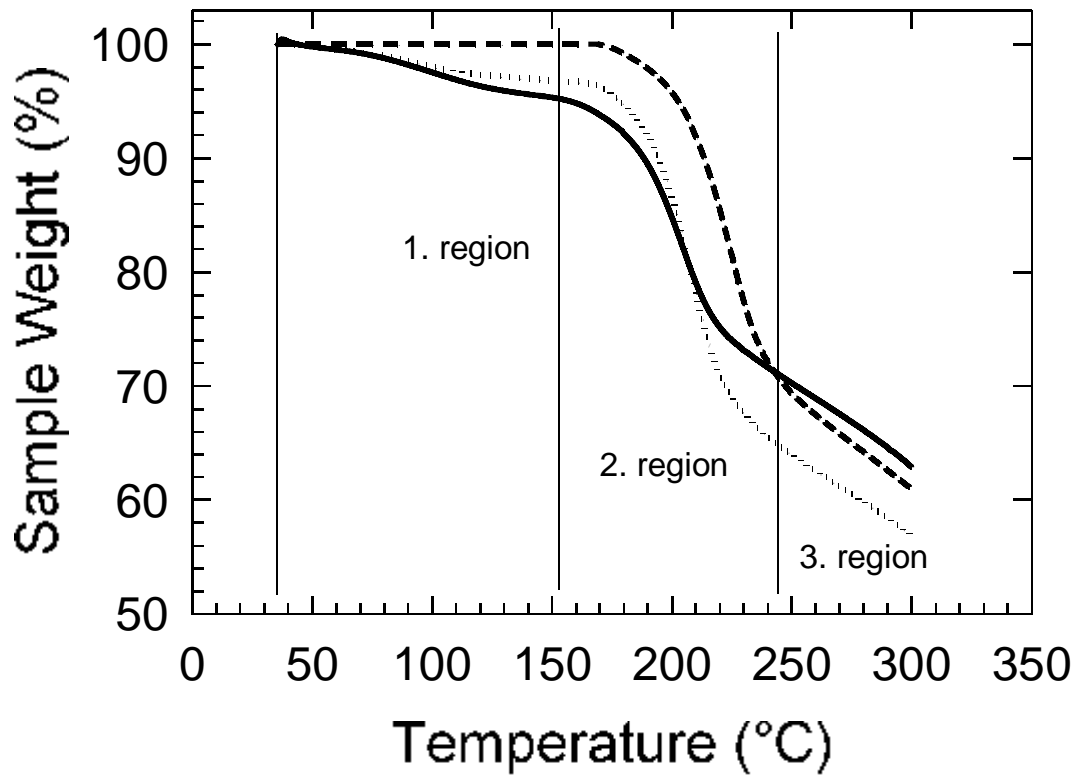


Figure 2. Thermogravimetric analysis of studied powder milk products: full line – powdered skimmed milk, dotted line powdered whey, short dashed line – demineralised powdered whey.

Figure(s)

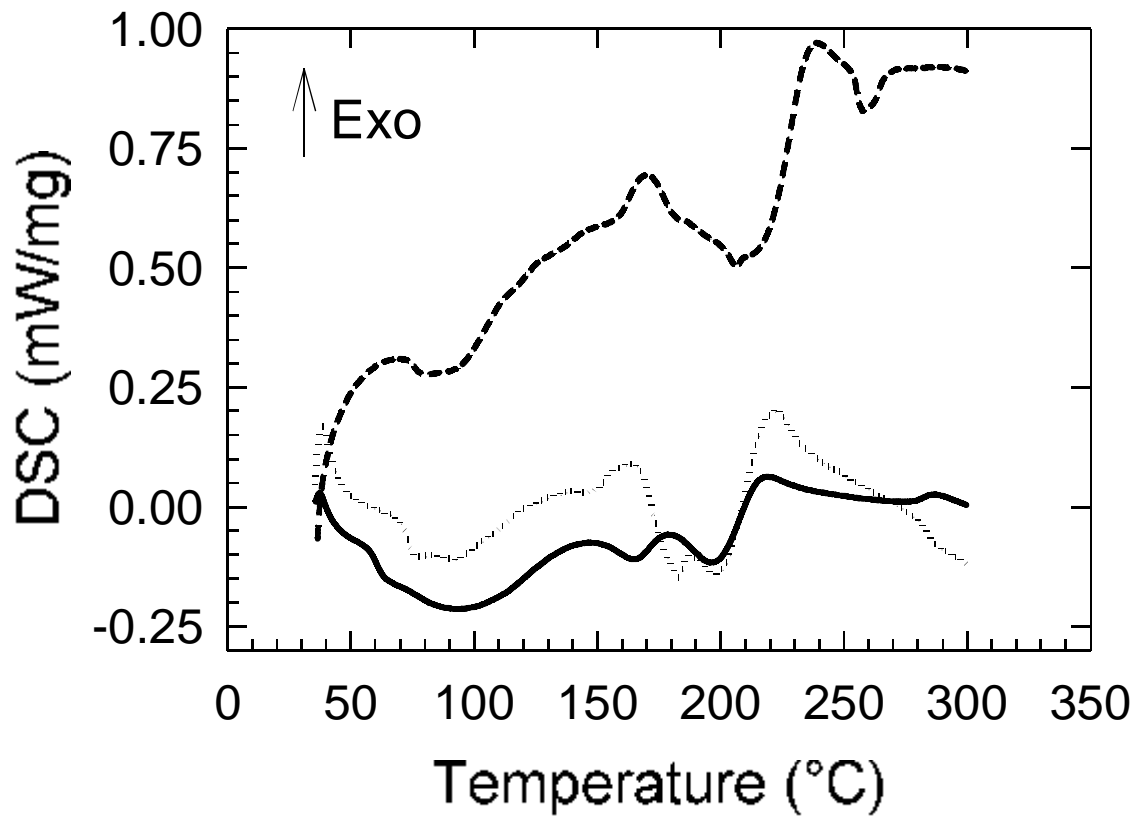


Figure 3. DSC pattern of studied powder milk products: full line – **powdered** skimmed milk, dot line – **powdered** whey, short dashed line – demineralised **powdered** whey.

Figure(s)

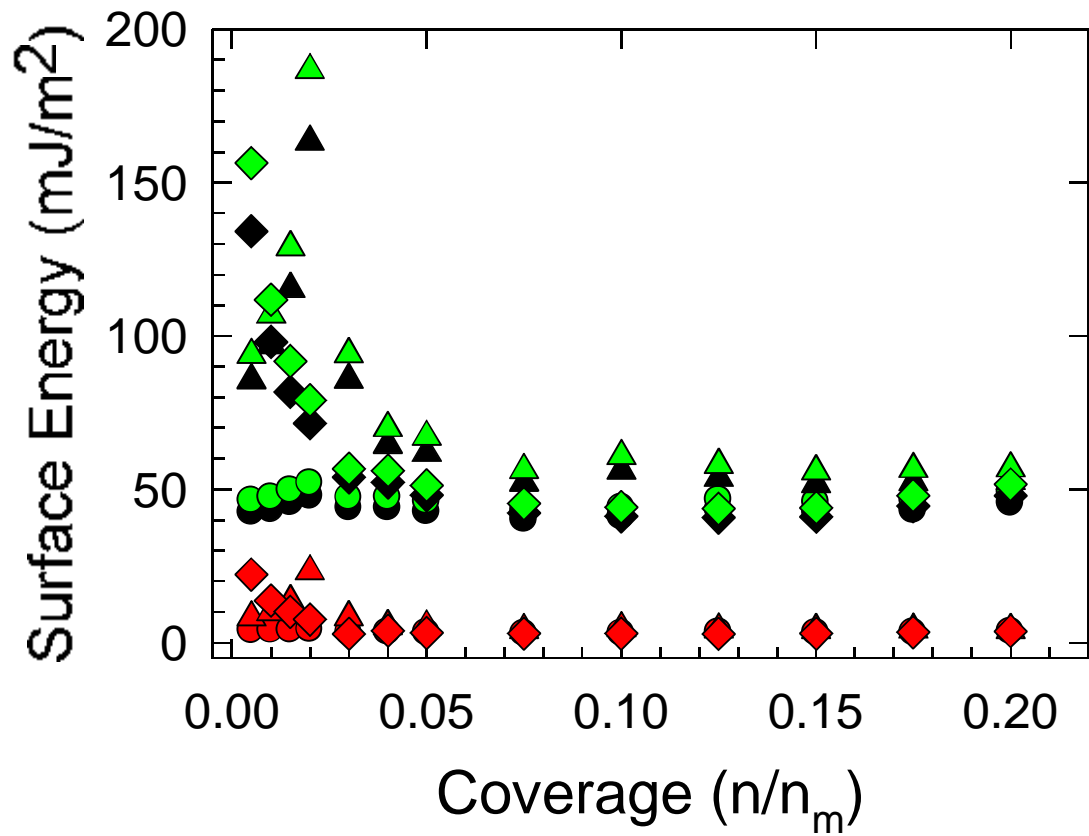


Figure 4. Surface energy and its **component** profiles of **powdered** milk products: circle – **powdered whey**, **triangle** – demineralised **powdered whey**, diamond – **powdered skimmed milk**, **black**– dispersive component of the surface energy (SFE), **red** polar component of SFE, **green** colour – total SFE.

Figure(s)

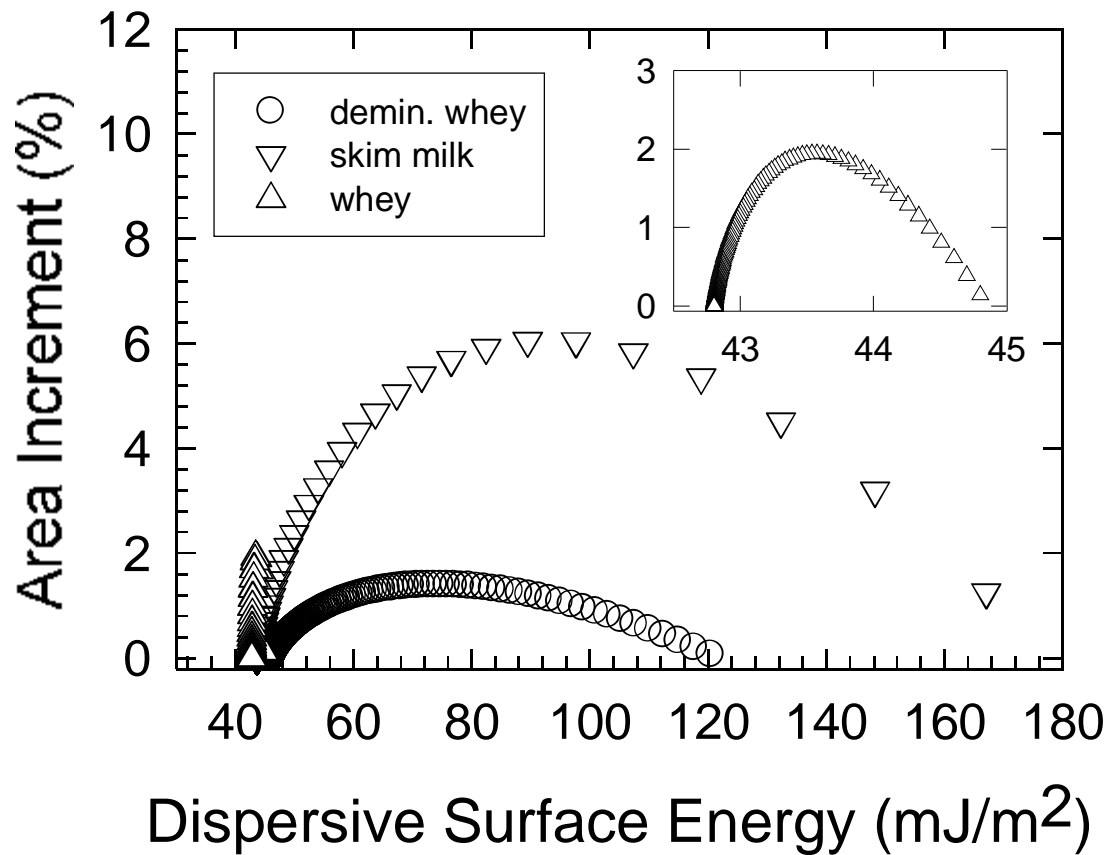


Figure 5. Dispersive surface energy distribution of demineralised powdered whey (circle), powdered skimmed milk (triangle down) and powdered whey (triangle up). Inset: expanded dispersive surface energy distribution of whey sample.

Figure(s)

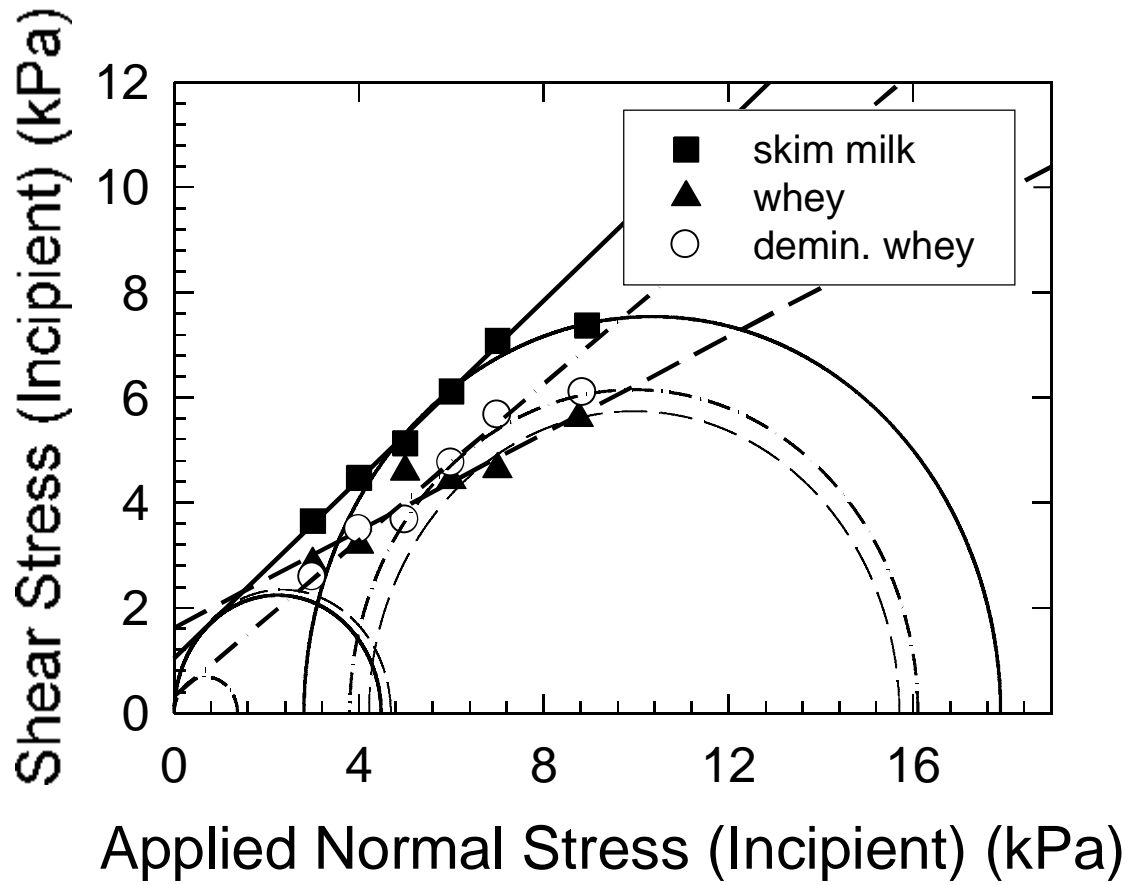


Figure 6. Yield locus and Mohr's circles of studied **powdered** milk products: full square **skimmed** milk, full triangle up – whey, empty circle – demineralised whey (measured at 24 °C).